Article Identifier
DOI: 10.22032/dbt.58733
URN: urn:nbn:de:gbv:ilm1-2023isc-023:5

60th ILMENAU SCIENTIFIC COLLOQUIUM
Technische Universität Ilmenau, 4 – 8 September 2023
URN: urn:nbn:de:gbv:ilm1-2023isc:1

ANALYSIS AND DEVELOPMENT OF A SENSOR CONCEPT FOR MULTISTABLE ACTUATORS WITH PASSIVE MAGNETIC SHAPE MEMORY ALLOY

Patrick Fleischmann M.Sc.[1], Julius Happel M.Sc.[2], Prof. Dr.-Ing. Bernd Gundelsweiler[1]

1) Institute of Design and Production in Precision Engineering, University of Stuttgart, Pfaffenwaldring 9, 70569 Stuttgart

2) ETO MAGNETIC GmbH, Hardtring 8, 78333 Stockach

ABSTRACT

Based on the current state of research, the aim of this paper is to develop a position sensor for actuators using passive magnetic shape memory alloys. The presented sensor concept converts the strain dependent permeability of the magnetic shape memory alloy into an inductance change by using a sensor coil arrangement. The change in inductance of the sensor coil is converted into a change in the resonant frequency of a parallel oscillating circuit. A microcontroller detects the resonant frequency of the circuit and converts it into a position sensor signal. To evaluate the functionality of the sensor, a test rig is developed that deforms the magnetic shape memory element under realistic application conditions. Experimental measurements in a climate chamber are used to evaluate the performance and characteristics of the sensor. The characteristic, temperature drift and hysteresis behavior are analyzed. It is proven that the presented sensor concept can be used to determine the position of passive magnetic shape memory alloy actuators.

Index Terms: Magnetic shape memory alloy, position sensor

1. INTRODUCTION

Due to the rising demand for energy efficient and highly integrated drives, novel actuator concepts are steadily gaining in interest. Through the passive use of magnetic shape memory (MSM) alloys as smart damping elements, these two requirements can be achieved. Conventional actuators can be transformed into multi-stable, energy-efficient drives by using the internal friction of passive magnetic shape memory alloys. [1,2] Depending on the composition of the alloy, stroke rates of between 6% and 12% can be achieved [3]. Additionally, the strain-dependent permeability of the alloy can be used to intrinsically determine the position of the actuator [4]. The combination in these properties enables the development of integrated, multi-stable and position-controlled mechatronic systems. These systems can for example be used advantageously in valve technology with applications ranging from hydrogen fuel cell technology to battery-powered medical devices. [1]
Based on the current state of research, this paper aims to develop a novel position sensor for actuators with passive magnetic shape memory alloys. First, a brief overview of the technical fundamentals of magnetic shape memory alloys is given. The sensor concept is then described and developed. In the subsequent characterization, the temperature behavior and hysteresis effects are investigated. Finally, the paper concludes with an application of the sensor in a push-pull actuator with a passive MSM element.

2. PERMABILITY-STRAIN BEHAVIOR OF MAGNETIC SHAPE MEMORY ALLOYS

The active material used in this sensor concept is a magnetic shape memory alloy, which is a martensitic single crystal with tetragonal unit cells. The specific alloy composition results in high transformation temperatures of up to 80 °C, making it suitable for passive valve applications. [1,5] The material is available as a bulk sample with a tetragonal geometry and will be abbreviated in the following as MSM element. The shape and dimensions of the MSM element are shown in **Figure 1**.

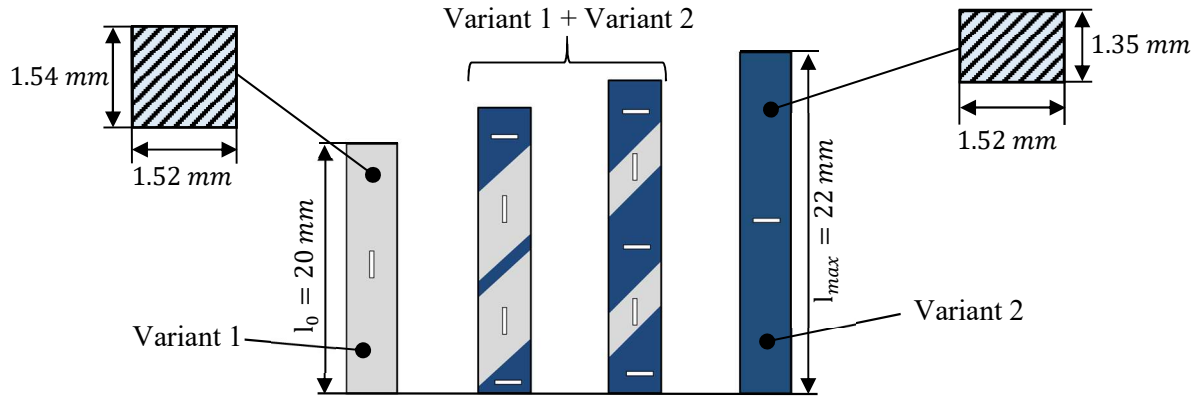

Figure 1: Variants of martensite according to the elongation state of the MSM element

The material usually exists in two martensite variations, each characterized by a different orientation of the martensite lattice. The martensitic lattice edge length is not equal in all three dimensions. Variant 1 has a smaller size in the Z-direction but a larger size in the Y-direction. Variant 2 has a larger extension in the Z-direction and hence a smaller extension in the Y-direction. The edge length in the X-direction is the same for both variants. The distribution of the variants and the associated macroscopic change in length of the MSM element can be manipulated by mechanical or magnetic stress induced reorientation of the unit cells. [4] The length change for the presented sensor concept is achieved by an external actuator force and is up to 12 % [3]. The external force must overcome the internal friction caused by the movement of the twin boundaries between the variants to deform the MSM element. For the following considerations it is simplified and assumed that there are only two strain states. In state 1 the MSM element is fully compressed and the crystal is only present in variant 1, whereas in state 2 the element is fully elongated and only the second variant is present. [4] **Figure 2** shows the two states with their respective permeabilities. These will be examined in more detail below.

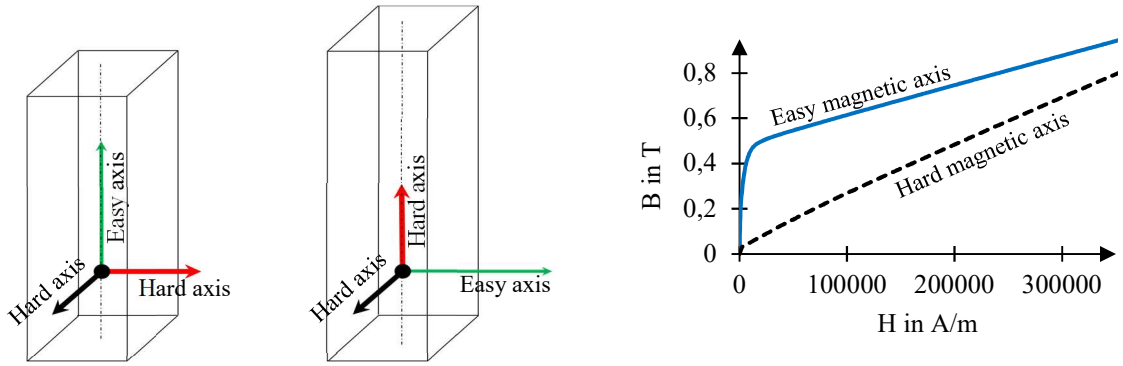

Figure 2: Permeability-strain behavior of a tetragonal shaped MSM element

In addition to the mechanical properties, the MSM element is characterized by magnetic anisotropy resulting from the magnetic properties within the unit cells of the particular martensite variant. A unit cell has a soft and a hard magnetic axis, where the soft magnetic axis is characterized by a high magnetic permeability and the hard axis by a low magnetic permeability. Due to the presence of the different variants, this property can be transferred to the whole MSM element, where it has a comparatively high permeability in the Z-direction in the fully compressed state and a significantly lower permeability in the fully stretched state. [4] This behavior is illustrated in **Figure 2** by the length of the magnetization axes for the two strain states. The strain-dependent change in the Z-direction permeability of the MSM element is measured in the following section using a cylindrical sensor coil arrangement.

3. SENSOR DESIGN

The concept behind this sensor is to exploit the change in permeability of the MSM element as a function of its deformation state. As can be seen from the magneto-mechanical properties in the previous chapter, the effective magnetic permeability μ_{MSM} of the entire MSM element has a direct correlation with the strain state. This characteristic provides the basic principle of the sensor system investigated in this study. For the technical application of the described variable magnetic properties of the MSM element, a concept is designed in which the MSM element forms the core of a thin cylindrical copper coil. The longitudinal axes of the coil and the MSM element coincide. This arrangement translates the change in permeability into a change in inductance of the sensor coil. **Figure 3** schematically shows the structure of the sensor system with the MSM element inserted.

1	MSM element
2	Sensor coil
3	Actuator armature
4	Fixed clamping

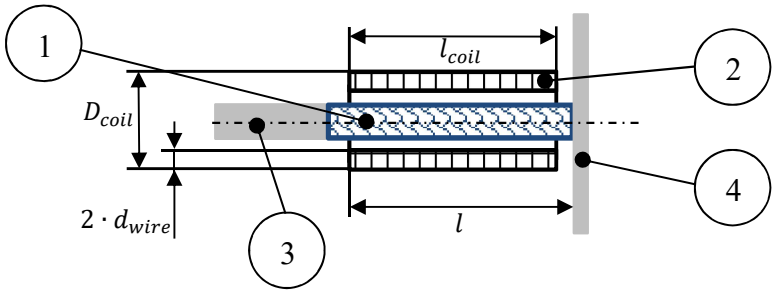

Figure 3: Sensor coil arrangement and corresponding design parameters

The approximate inductance L of the cylindrical sensor coil is given by equation 1. Where N is the number of turns of the coil, μ_0 is the magnetic field constant and l_{Coil} is the length of the sensor coil. Besides these constants, the coil inductance L depends on the cross-section $A_{MSM}(l)$ and the effective magnetic permeability $\mu_{MSM}(l)$ of the coil core. For the MSM alloy used, the total length l varies between $l_0 = 20\ mm$ and $l_{max} = 22\ mm$. The cross-sectional area can be calculated from the deformation length l and the constant volume of the MSM element.

$$L = f(\mu_{MSM}(l),\ A_{MSM}(l),\ l_{Coil},\ N^2,\ \mu_0)\ \ with\ l_0 \leq\ l\ \leq l_{max} \qquad (1)$$

To quantify the sensor effect, a two-layer coil is wound with a fixed number of turns $N = 190$ and $d_{wire} = 0.15\ mm$. The copper winding is supported by an additively manufactured cylindrical coil body, which guides the MSM element and prevents it from buckling. The material of the coil body is a polyamide polymer, which is diamagnetic and therefore has a negligible effect on the coil inductance. The sensor effect is quantified by measuring the inductance of the sensor coil using an impedance analyzer (WAYNE KERR, 3255B). In general, the inductance

of the coil shows a dependence on the measurement frequency. This dependence is mainly caused by eddy current effects of the coil winding and the MSM based core. The inductance measurement is performed at a constant frequency $f_{meas} = 500\ kHz$ to ensure comparability between different measurement configurations. The frequency chosen depends on the electrical system being evaluated. The measurement results are summarized in **Table 1.**

Table 1: Verification of the effect of the sensor by measurement

Coil inductance at different core configurations ($f_{meas} = 500\ kHz$)			Relative inductance change $\frac{L_{MSM}(20\ mm) - L_{MSM}(22\ mm)}{L_{MSM}(20\ mm)} * 100\%$
L_{Air}	$L_{MSM}(22\ mm)$	$L_{MSM}(20\ mm)$	
37.05 µH	40.48 µH	53.00 µH	23.6 %

The inductance is measured with the coil core removed, at maximum extension and with the MSM element fully compressed. In the expanded state the length of the MSM element is $l_{max} = 22\ mm$, in the compressed state the length of the MSM element is $l_0 = 20\ mm$. For each of these coil core configurations, the inductance is measured and the relative change between the compressed and expanded states is determined.

4. SENSOR ELECTRONICS AND TEST SETUP

This section presents an electronic measurement concept and system for evaluating the sensor. This system allows dynamic measurement of the coil inductance. In general, the purpose of the measurement electronics is to convert a given change in permeability into a change in the inductance of the sensor coil for use in engineering applications. In this paper, an indirect inductance measurement using an LC oscillating tank circuit is developed, taking into account sensor dynamics, complexity and cost efficiency. A systematic overview of the electronic concept described below is shown in **Figure 4**.

1	Transducer
2	Sensor coil with MSM element
3	Embedded measurement system
4	LC tank
5	Signal processing
6	Microcontroller

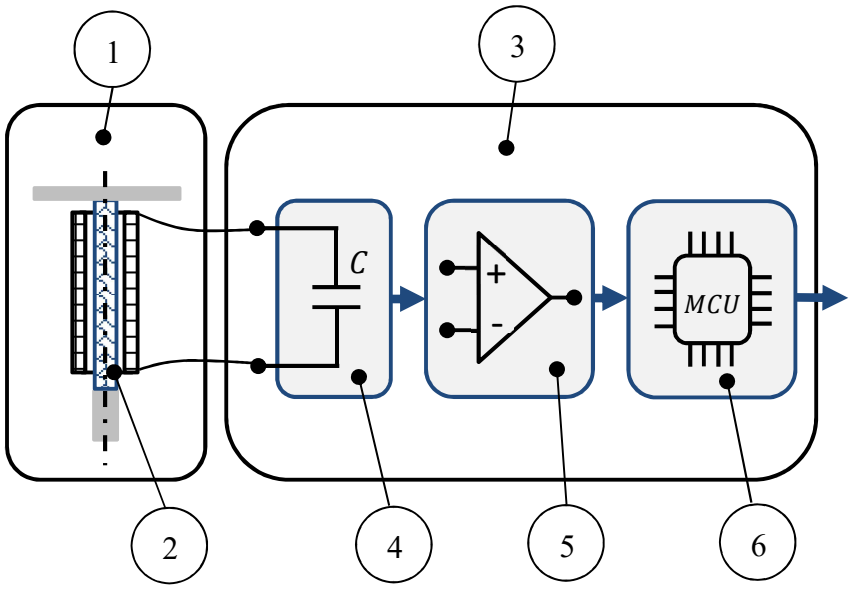

Figure 4: Systematic overview of the sensor concept

The measurement system can be divided into three functional blocks. The first block represents the parallel LC tank circuit. In this approach, the parallel tank circuit is formed using the inductance of the sensor coil and a capacitance. This resonant tank is driven by a differential amplifier to form a self-excited oscillator. The advantages of this oscillator circuit are its simple design, the sinusoidal output waveform and the dependence of the oscillation frequency solely on the reactive components of the parallel resonant tank. After start-up, the circuit oscillates at the resonant frequency of the parallel tank. With the strain-dependent inductance L and constant capacitance C, the resonant frequency f_R is estimated by the simplified Thomson oscillation equation (2).

$$f_R = \frac{1}{2 \cdot \pi \cdot \sqrt{L \cdot C}} \tag{2}$$

The direct dependence of the resonant frequency on the inductance is the fundamental operating principle of the transmitter developed in this paper. A displacement dependent resonant frequency can be generated by the sensor coil. From equation (1) and equation (2) the correlation between the resonant frequency and the inductance can be determined theoretically by equation (3).

$$f_R(l) = \frac{1}{2 \cdot \pi \cdot \sqrt{f(\mu_{MSM}(l),\, A_{MSM}(l),\, l_{Coil},\, N^2,\, \mu_0) \cdot C}} \tag{3}$$

The signal processing in the second block has the task of converting the sinusoidal signal from the oscillator circuit into a square wave signal with constant amplitude. This conversion is achieved by a high-speed comparator circuit. The third block is the evaluation unit, which includes a microcontroller (Microchip, ATMega328p) that captures the frequency of the square wave signal by counting periods in a fixed time interval. The measured frequency is then converted to a proportional strain/armature position of the target application.
In order to evaluate and characterize the entire sensor system, a test setup is now presented with which the measurements presented in chapter 5 are carried out. The test setup is driven by a high-precision linear axis (Physik Instrumente, M-227.25), which enables controlled stretching and compression of the MSM element. The MSM element is inserted in the sensor coil shown in chapter 3 and is connected to the linear actuator via welded flanges on the top and bottom faces. The entire test setup is enclosed in a climate chamber (Weisstechnik, ClimeEvent C/340/70a/3) where the ambient temperature is maintained between $T_{amb} = -15\,°C$ and $T_{amb} = -60\,°C$. The test setup is shown schematically in **Figure 5**.

1	Climatic chamber
2	MSM sensor
3	Test rig with linear actuator
4	Electronic system

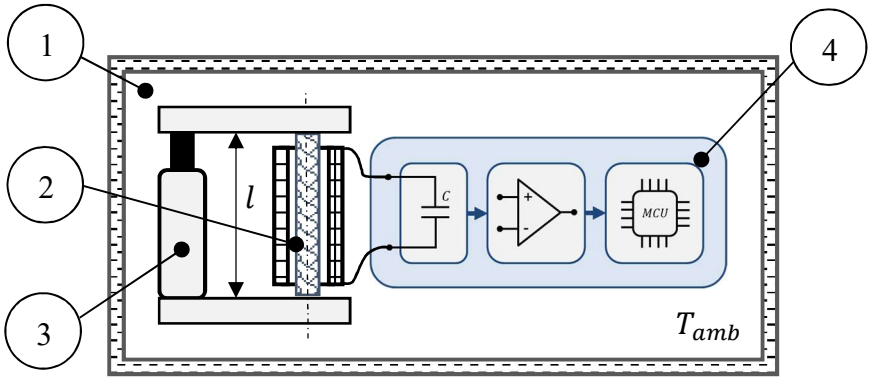

Figure 5: Test setup of the entire sensor system

To choose the capacitance C, a study is carried out by determining the LC tank circuit resonant frequencies for the two deformation states for different capacitances. **Figure 6** shows the resonant frequencies as a function of capacitance.

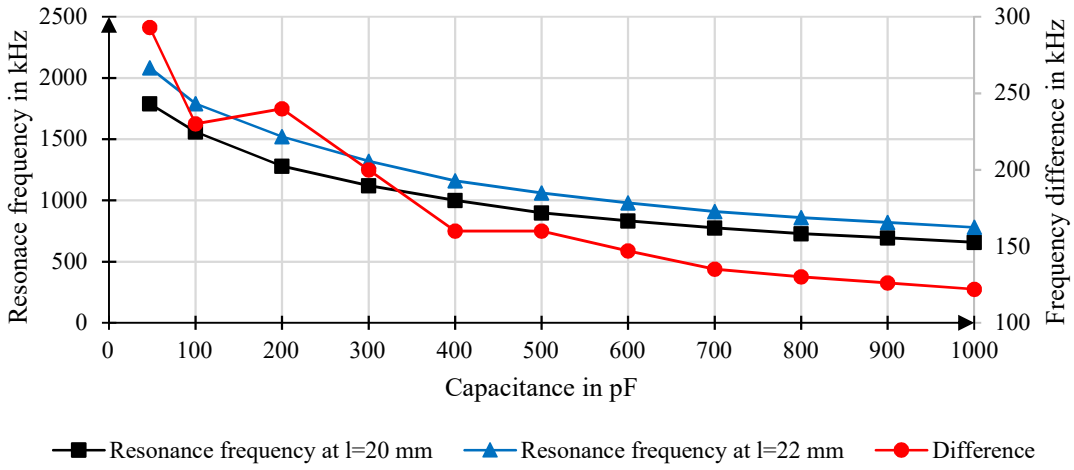

Figure 6: Dependence of the resonance frequency on the capacitance

In order to choose a suitable capacitance, the difference between the fully expanded and fully compressed resonant frequencies is calculated as the next step. The maximum value of this difference is obtained for a capacitance of C = 47 pF and is therefore fixed for the following evaluation. Smaller values were not tested due to the maximum measurement frequency of the electronics.

5. EVALUATION

The quantitative evaluation of the developed sensor system is presented in the current section. The first step in the evaluation is to determine the sensor characteristic for an ambient temperature of 20 °C. This is done by elongating and compressing the MSM element between 20000 µm and 21800 µm (step size 100 µm) using the test setup shown in **Figure 5**. This measurement is carried out 5 times with results depicted in **Figure 7**.

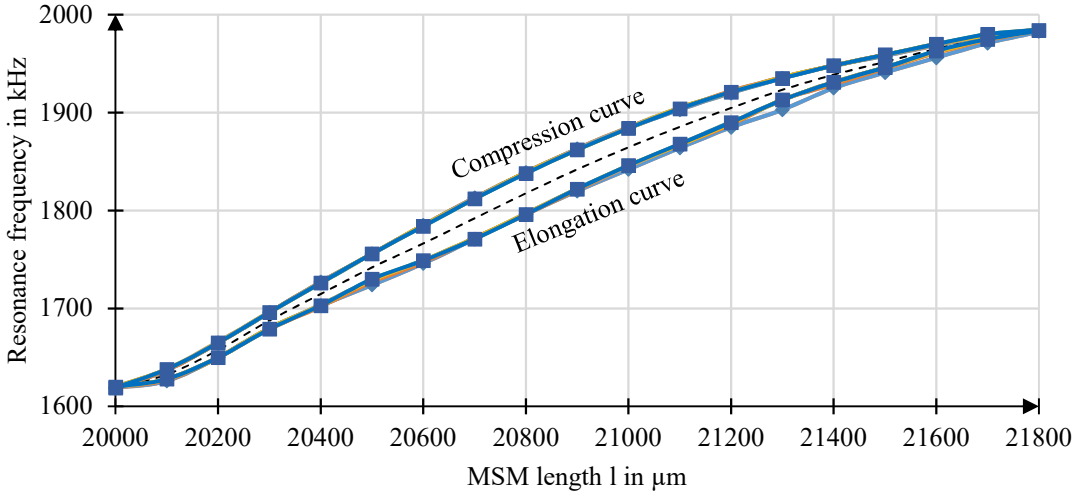

Figure 7: Characteristic sensor curves at 20 °C

It can be seen that an elongation cycle of 1800 µm is mapped at approximately 365 kHz, where the resonant frequency f_R increases with increasing strain. This behaviour is explained by the effective permeability being minimal in the fully elongated state and maximal in the fully compressed state. It can be seen that all 5 cycles of strain fit very precisely over each other and the variation is small. A hysteresis forms between the elongation and compression curves, which amounts to approx. 40 kHz on average. It should be noted that a different sample of MSM element is used for the measurement than before and therefore there are slight variations between the maximum difference in frequency from the measurement in **Figure 6** and the characteristic curve in **Figure 7**.

5.1 Hysteresis behavior under different ambient temperatures

In the context of a real technical application as a sensor component in a multistable MSM fluid valve, the hysteresis behavior is analyzed in detail under the influence of different ambient temperatures (T= -15 °C, T=0 °C, T=20 °C, T=40 °C, T=60 °C). The hysteresis of the system is the difference between the output value (resonant frequency f_R) of the sensor during the rise and fall of the input variable (level of strain). This difference can occur due to delayed responses of the system. In the case of the developed position sensor, the hysteresis corresponds to the difference of the resonance frequencies of the push and pull characteristics at the MSM length l and is calculated according to equation (4). **Figure 8** shows the calculated hysteresis over the strain for a range of ambient temperatures, where the temperature range is restricted by the transformation temperature of the MSM alloy.

$$Hyst(l) = f_{R_{push}}(l) - f_{R_{pull}}(l) \quad with \quad f_{R_{push}}(l) \neq f_{R_{pull}}(l) \tag{4}$$

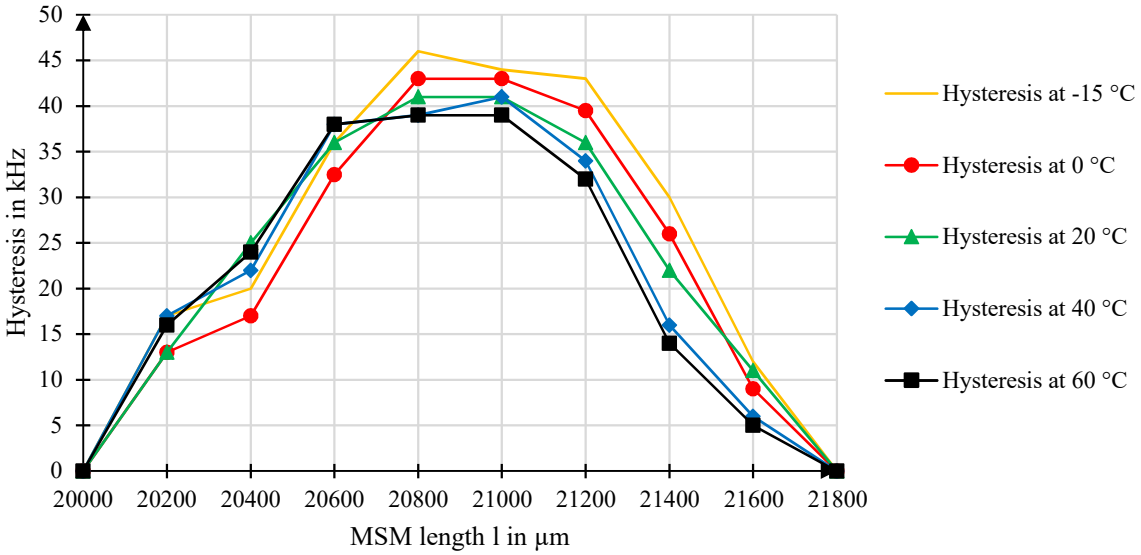

Figure 8: Temperature dependent hysteresis behavior

In addition to the maximum hysteresis level, this measure provides a qualitative evaluation of the symmetry of the sensor curve at different ambient temperatures. It can be seen that the shape of the curve is similar for all the temperatures tested and furthermore the variation between the curves is minor compared to the maximum hysteresis. This suggests that the shape of the sensor curve has a low dependence on ambient temperature, which simplifies the compensation process.

5.2 Temperature drift

Further the drift of sensor outputs at different temperatures is considered. The entire test set-up (shown in **Figure 5)** is located inside the climate chamber for measuring. To measure, the linear actuator is used to elongate and compress the MSM element at different ambient temperatures (T=-15 °C, T=0 °C, T=20 °C, T=40 °C, T=60 °C). It is ensured that the entire system is in thermal steady state between the different measurements. For clarity, only the extreme values of the sensor output are plotted versus ambient temperature**. Figure 9** shows the resonance frequency f_R for the maximum and minimum MSM length.

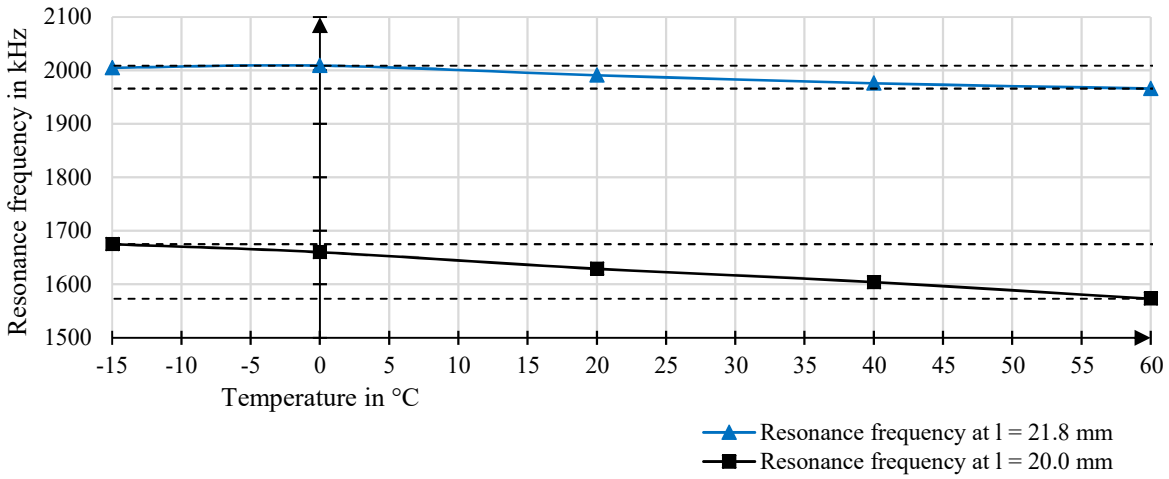

Figure 9: Temperature drift of sensor values

Figure 9 shows the following behavior, the characteristic curve of the sensor shifts downwards as the temperature rises, whereby the amplitude of the characteristic curve is significantly greater than the temperature-related drift. From this measurement, a compensation table can be created that matches the shown drift to the actual ambient temperature.

6. APPLICATION

To demonstrate the function and performance of the concept in a real application, the sensor system is integrated into a multistable position controlled push-pull solenoid actuator equipped with a laser triangulation sensor (Micro Epsilon, ILD1220-50). **Figure 10** shows the schematic arrangement.

1	MSM sensor
2	Laser triangula-tion sensor
3	Push pull actuator
4	Actuator armature

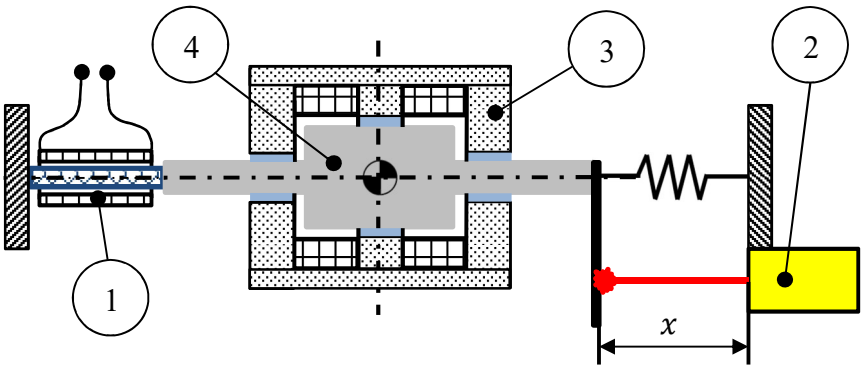

Figure 10: Push pull MSM solenoid actuator equipped with multiple position sensors

To demonstrate the functionality, the actuator is operated in a cyclic rectangular motion profile. The position is controlled by the laser triangulation sensor. The MSM based sensor system is operated in parallel. Both sensors are read simultaneously by a microcontroller (sampling frequency = 1 kHz) and output through its digital-to-analogue converter. **Figure 11** shows the profile of the target position, the signal from the laser triangulation sensor and the signal converted from the MSM-based sensor system. The difference between the two sensor signals is also determined and plotted as an error plot.

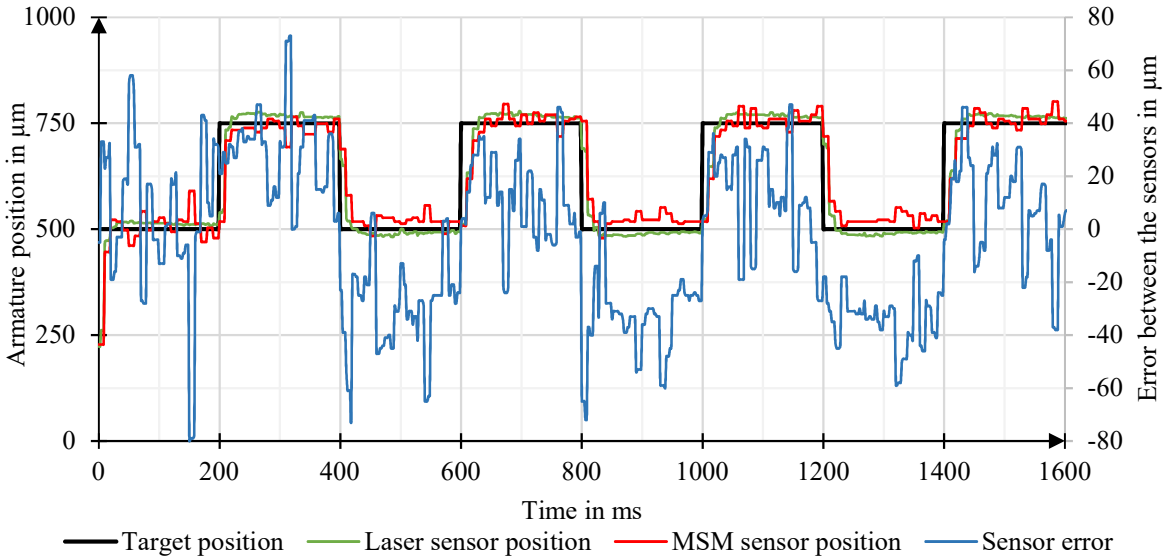

Figure 11: Comparison of the sensors in a position controlled application

Based on **Figure 11**, it can be concluded that the position sensor developed in this paper is fully functional and reproduces the armature position of the actuator analogously to the laser triangulation sensor. In particular, the dynamics of the two sensors are very similar and there are no significant delay effects. The resulting error between the two sensor signals is caused by the hysteresis mentioned in chapter 5. The error can be reduced by a proper hysteresis compensation strategy.

7. CONCLUSION

In conclusion, it has been shown how a sensor concept for applications with passive MSM elements can be designed to take advantage of the strain-dependent permeability. The concept introduced converts the change in permeability into a change in inductance via a simple and low-cost sensor coil arrangement. It has been proven by inductance analyzer measurement that the change in inductance is in the double-digit percentage range and can therefore be used for technical applications. In order to be able to evaluate the inductance change dynamically and easily, an electronic system was developed in which the inductance change is converted into a resonance frequency change by means of an LC resonance tank circuit. The frequency measurement and conversion to a position signal is handled by a low-cost microcontroller. After developing the sensor hardware, the sensor characteristic was measured using a test rig. The entire system was then characterized at different ambient temperatures. It was shown that the system has a dependence on ambient temperature in terms of maximum values and hysteresis. However, the characteristics and quality of the sensor signal are retained. In the final chapter, a comparison was made between a commercial laser triangulation sensor and the MSM-based

sensor using a controlled actuator application. With this application, the functionality could be conclusively proven. In future work on the sensor concept, the sensitivity of the sensor coil will be optimized using FEA. A compensation strategy to reduce errors caused by the influence of the ambient temperature and the characteristic hysteresis will then be implemented.

8. REFERENCES

[1] J. Happel, R. Schnetzler and M. Laufenberg, „Multistable valve technology with magnetic shape memory alloy as passive element activated by a bidirectional solenoid actuator," in *12th International Fluid Power Conference (IFK)*, vol.3, pp. 315-320, October 12-14, 2020, Dresden, Germany.

[2] H.D. Stölting, E. Kallenbach and W. Amrhein, *Handbuch Elektrische Kleinantriebe.* Munich, Germany: Carl Hanser Verlag, 2011.

[3] A. Sozinov, N. Lanska, A. Soroka, and W. Zou, "12% magnetic field-induced strain in Ni-Mn-Ga-based non-modulated martensite" in *Applied Physics Letters,* vol.102 (2), January 2013.

[4] I. Suorsa, E. Pagounis and K. Ullakko, „Position dependent inductance based on magnetic shape memory materials" in *Sensors and Actuators A: Physical,* vol.121, pp. 136-141, May 31, 2005.

[5] E. Pagounis, R. Chulist, T. Lippmann, M. Laufenberg, W. Skrotzki, "Structural modification and twinning stress reduction in a high-temperature Ni-Mn-Ga magnetic shape memory alloy" in *Applied Physics Letters,* vol.103 (11), September 2013

CONTACTS

Patrick Fleischmann M.Sc. email: patrick.fleischmann@ikff.uni-stuttgart.de

Julius Happel M.Sc. email: j.happel@etogruppe.com

Prof. Dr. -Ing. Bernd Gundelsweiler email: bernd.gundelsweiler@ikff.uni-stuttgart.de